Environmental Science & Technology

pubs.acs.org/est

Article

Critical Role of Semiquinones in Reductive Dehalogenation

Srinidhi Lokesh, Myron L. Lard, Robert L. Cook, and Yu Yang*

Cite This: https://doi.org/10.1021/acs.est.3c03981

Read Online

ACCESS | Metrics & More | Article Recommendations | Supporting Information

ABSTRACT: Quinones and products of their redox reactions (hydroquinones and semiquinones) have been suggested as important players in the reductive dehalogenation of organohalogens mediated by natural and pyrogenic organic matter, although based on limited direct evidence. This study focused on the reductive dehalogenation of a model organohalogen (triclosan) by 1,4-benzohydroquinone (H_2Q). In the presence of H_2Q only, degradation of triclosan does not occur within the experimental period (up to 288 h); however, it takes place in the presence of H_2Q and $FeCl_3$ under anoxic conditions at pH 5 and 7 (above the pK_a of SQ = 4.1) only to be halted in the presence of dissolved oxygen. Kinetic simulation and thermodynamic calculations indicated that benzosemiquinone (SQ^-) is responsible for the reductive degradation of triclosan, with the fitted rate constant for the reaction between SQ^- and triclosan being 317 M^{-2} h^{-1}. The critical role of semiquinones in reductive dehalogenation can be relevant to a wide range of quinones in natural and engineering systems based on the reported oxidation−reduction potentials of quinones/semiquinones and semiquinones/hydroquinones and supported by experiments with additional model hydroquinones.

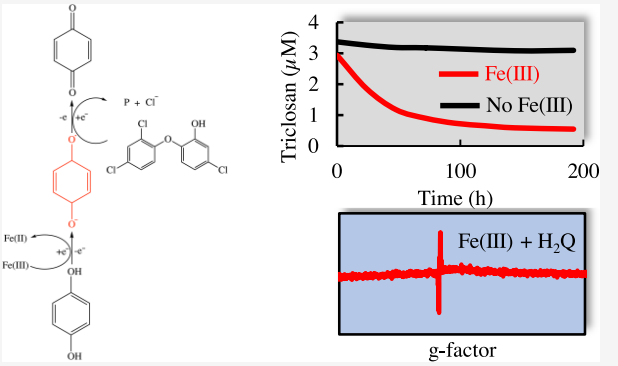

KEYWORDS: *semiquinone, dehalogenation, thermodynamic calculation, rate constant, organohalogen*

Downloaded via Yu Yang on September 5, 2023 at 13:57:52 (UTC).
See https://pubs.acs.org/sharingguidelines for options on how to legitimately share published articles.

INTRODUCTION

Enhancement of dehalogenation is important for natural attenuation, remediation, and the engineering treatment of wastewater. Natural organic matter (NOM) and pyrogenic compartments (including black carbon, activated carbon, and biochar) can promote dehalogenation by accelerating electron transport.[1−3] Previous studies have attributed the redox reactivity of NOM and biochar to their quinone (QN) components (aromatic domain with conjugated dione structure), but there is limited direct evidence.[4−7] In an effort to understand the reactivity of the quinone system using model quinones, Perlinger et al.[8] showed that the hydroquinone form of juglone, namely, mercaptojuglone, was able to reduce pentachloroethane in the presence of hydrogen sulfide, with a first-order rate constant of 9×10^{-3} h^{-1}. For semiquinone (SQ) radicals generated via the reduction by *Geobacter metallireducens* in humic substances, Scott et al.[4] quantitatively demonstrated a relationship between the amount of SQ radicals and the electron-accepting capacity of humic substances. Findings by Xu et al.[9] that biochar could increase the microbial reduction of hematite through QN-involved reactions were supported by the electron paramagnetic resonance (EPR) signals for SQs in biochars.

Due to the difficulty in quantifying quinones in NOM or biochar beyond EPR analysis of semiquinones (thermodynamically a minor fraction of all quinones under normal conditions), their redox reactivities have been demonstrated using model quinone compounds as analogues. Anthraquinone-2,6-disulfonate (AQDS) has been widely used as an analogue for quinones in NOM to demonstrate their reactions with various electron acceptors, such as ferric minerals.[10−12] Jiang et al.[13] studied the reactions between 1,4-benzohydroquinone (H_2Q) and Fe(III) in the solution phase and determined that H_2Q can be reversibly oxidized by Fe(III) with a reaction rate constant determined using a kinetic model. Based on studies using a range of model QNs, O'Loughlin[14] demonstrated a relationship between the reaction rate constant for quinone-mediated microbial reduction of lepidocrocite and the oxidation−reduction potentials of quinones. While model quinones have been used to study the redox reactivity mediated by these species, rare studies have been devoted to directly demonstrating the reactions between organohalogen and quinones.

This study examined the reactions between a model organohalogen, triclosan, and H_2Q (Supporting Information (SI), Figure S1). Rate constants for the critical reactions were determined by mathematical fitting of the reaction kinetics, assuming first order for all reactants. Thermodynamic calculations were used to determine the equilibrium concen-

Received: May 26, 2023
Revised: August 11, 2023
Accepted: August 14, 2023

ACS Publications © XXXX American Chemical Society

Table 1. Key Reactions and Rate Constants at pH 5 Considered for the Kinetic Fitting[a]

no.	reaction		rate constant (M^{-1} s^{-1}/$M^{-2}S^{1-}$)	refs
1	$Fe^{3+} + H_2Q \overset{k1,k-1}{\Longleftrightarrow} SQ^- + Fe^{2+} + 2H^+$	$k1$	1×10^3	28
		$k-1$	9×10^6	13
2*	$SQ^- + Fe^{3+} \overset{k2,k-2}{\Longleftrightarrow} Q + Fe^{2+}$	$k2$	$\leq 1 \times 10^5$	29
		$k-2$	$\leq 1 \times 10^3$	30
3	$2SQ^- + TCS + H^+ \overset{k3}{\rightarrow} 2Q + Cl^- + P$	$k3$	317	this study
4*	$2SQ^- + 2H^+ \overset{k4,k-4}{\Longleftrightarrow} H_2Q + Q$	$k4$	$\leq 1 \times 10^{10}$	29,30
		$k-4$	$\leq 1 \times 10^7$	
5	$SQ^- + O_2 + H^+ \overset{k5,k-5}{\Longleftrightarrow} Q + HO_2^\bullet$	$k5$	1×10^3	36,38
		$k-5$	1.9×10^7	33
6	$HO_2^\bullet + HO_2^\bullet \overset{k6}{\rightarrow} H_2O_2 + O_2$	$k6$	2.5×10^7	34
7	$SQ^- + HO_2^\bullet + H^+ \overset{k7}{\rightarrow} H_2Q + O_2$	$k7$	5×10^8	10
8	$Fe^{3+} + HO_2^\bullet \overset{k8,k-8}{\Longleftrightarrow} Fe^{2+} + O_2 + H^+$	$k8$	2.5×10^6	35
		$k-8$	1.3	13
9	$Fe^{2+} + HO_2^\bullet + H^+ \overset{k9}{\rightarrow} Fe^{3+} + H_2O_2$	$k9$	6.6×10^6	35

[a]P denotes the triclosan degradation byproduct; *as there is a lack of rigorously constricted values for the rate constants of these reactions, they were not accounted for in the mathematical fitting of this study.

trations of benzosemiquinone (SQ^-) and compared to kinetic simulations. Finally, additional model hydroquinones were reacted with triclosan to validate the ubiquitous prominent role of semiquinones in the reductive dehalogenation of triclosan.

METHODS AND MATERIALS

Materials. The standard compound of triclosan (purity ≥98%) was purchased from Sigma-Aldrich (St. Louis, MO). 1,4-Benzoquinone (purity ≥98%) (Q) was purchased from Alfa Aesar (Haverhill, MA). Model hydroquinones, including benzohydroquinone (H_2Q) (purity ≥99%), dimethyl hydroquinone (purity ≥99%), trimethyl hydroquinone (purity ≥99%), 1,2-dihydroxylnaphthlene (purity ≥99%), mitoxantrone (purity ≥97%), and epigallocatechin (purity ≥95%), were obtained from Sigma-Aldrich. $FeCl_2$ and $FeCl_3$ (purity ≥99%) were purchased from Sigma-Aldrich. All other chemical reagents used in this study were of analytical grade.

Redox Reactions. Triclosan was reacted with H_2Q in the presence and absence of oxygen (O_2) at room temperature. For the reaction in the absence of O_2, the reaction solution was bubbled with compressed N_2 (purity of >98.5%, Praxair, Danbury, CT) for 6 h. Our tests showed that the dissolved O_2 concentration reduced to less than 1 μM after this process, measured by a dissolved oxygen probe (Seven2Go DO meter S4, Mettler Toledo, Columbus, OH). Thereafter, the solution was transferred into an anoxic glovebox (~100% N_2) (Coy, Grass Lake, MI). Reactions in the presence of O_2 were conducted under ambient air, where the dissolved O_2 was measured to be constant at ~200 μM. To demonstrate the role of SQ^-, the reaction was also conducted in the presence of $FeCl_3$, as previous studies have documented the oxidation of H_2Q by Fe(III).[13,15,16] At various time points, solutions were sampled for analysis. Experiments were conducted in triplicate.

To get a reliable kinetic fitting for the reductive degradation of triclosan without concerns for the generation of byproducts and their consumption for H_2Q/SQ^- in the kinetic simulation, additional experiments at pH 5 were conducted with low concentrations of triclosan (0.15, 0.2, and 0.3 μM) in the presence of 20 μM Fe(III) and H_2Q with and without O_2. The impact of the initial concentration of H_2Q was also examined by reacting 200 μM H_2Q with 20 μM $FeCl_3$ and 0.2 μM triclosan. For these reactions, the residual concentration of triclosan was analyzed at different intervals along with the concentrations of H_2Q, Q, and Fe(III)/Fe(II). Following the same protocol, additional hydroquinones (dimethyl hydroquinone (DMH), trimethyl hydroquinone (THM), and 1,2-dihydroxylnaphthlene (DHN)) were reacted with triclosan and Fe(III) with initial concentrations for HQ/triclosan/Fe(III) of 3/3/3 and 3/3/0 μM, in the presence and absence of dissolved O_2. To verify the reaction for more widely used hydroquinones and naturally occurring hydroquinones, mitoxantrone—widely used in cancer treatment,[17−19] and epigallocatechin—the most abundant catechin found in tea,[20−23] were reacted with triclosan and Fe(III), with initial concentrations for hydroquinone/triclosan/Fe(III) of 3/3/3 and 3/3/0 μM, in the presence and absence of dissolved O_2 (Table S1). The Fe(III) concentration used in this study (0.3−20 μM) is similar to environmentally relevant Fe concentrations found in oceans (0.07 ± 0.04−0.76 ± 0.25 nM),[24,25] rivers (8.9−17.9 μM),[26] groundwater (1.78 mM),[26] and porewater analysis of peatland soil (20 ± 10−1600 ± 300 μM).[27]

Chemical Analysis. Chemical analysis of triclosan, H_2Q, Q, and Fe(II) is detailed in Text S1 and Figure S3. In brief, triclosan, H_2Q, and Q were analyzed by high-performance liquid chromatography (HPLC) with a diode-array detector (DAD) for ultraviolet (UV) analysis. Triclosan degradation byproducts for the reaction samples of 20 μM H_2Q, 20 μM of Fe(III), and 0.3 μM of triclosan were analyzed with electrospray ionization-time-of-flight mass spectrometry (ESI-TOF-MS). Fe(II) was measured using the ferrozine method.[9]

Kinetic Simulation. The kinetics for the reactions of triclosan in the presence of H_2Q and $FeCl_3$ were fitted using Matlab 2020b (The Mathworks Inc.) with self-developed coding. Fitting and analysis are detailed in Table 1. Partial rate constants were sourced from the literature.[10,13,28−35] The least-squares fitting was conducted with the "fcn2optimexpr" toolbox. Several kinetic simulations/fittings were conducted in this study: (1) for the system of H_2Q and $FeCl_3$, based on the reported rate constant for the reactions between H_2Q and Fe(III),[13] the dynamics of Q/H_2Q/SQ^-, and Fe(III)/Fe(II)

https://doi.org/10.1021/acs.est.3c03981
Environ. Sci. Technol. XXXX, XXX, XXX−XXX

Table 2. Key Reactions Considered for Thermodynamic Calculation

mass balance equation of Fe

$$Fe(III)_T = [Fe^{3+}] + [Fe(OH)^{2+}] + [Fe(OH)_2^+] + [Fe(OH)_3(aq)] + [Fe(OH)_4^-] \quad (1)$$

$$Fe(II)_T = [Fe^{2+}] + [Fe(OH)^+] + [Fe(OH)_2(aq)] + [Fe(OH)_3^-] + [Fe(OH)_4^{2-}] \quad (2)$$

mass balance equation of the quinone system

$$Q_T = [Q] + [SQ] + [SQ^-] + [H_2Q] + [HQ^-] + [Q^{2-}] \quad (3)$$

electron balance equations

$$e_T = [SQ] + [SQ^-] + 2 \times ([H_2Q] + [HQ^-] + [Q^{2-}]) + Fe(II)_T \quad (4)$$

Nernst equations

$$E = E^0 + \frac{RT}{2F}\ln\left(\frac{[Q][H^+]^2}{[H_2Q]}\right) \quad (5)$$

$$E = E^0 + \frac{RT}{2F}\ln\left(\frac{[Fe^{3+}]}{[Fe^{2+}]}\right) \quad (6)$$

were calculated when triclosan was not included in this reaction theme; (2) for the system of H_2Q, $FeCl_3$, and triclosan, based on the reported rate constant for the reaction between H_2Q and Fe(III), the time-dependent concentration of triclosan was simulated based on the least-squares fitting with the rate constant for the reaction between SQ^- and triclosan fitted; and (3) for the system with initial 200/20/0.2 μM H_2Q, $FeCl_3$, and triclosan, in addition to dynamics of triclosan, the time-dependent concentrations of H_2Q/Q, Fe(III)/Fe(II) were also simulated.

Thermodynamic Calculation. The thermodynamic calculation was conducted through the resolution of equation groups (mass balance and electron balance) (by function 'fsolve') using Matlab 2020b (The Mathworks Inc.) with self-developed coding. Based on the theme developed in Uchimiya et al.,[36] the thermodynamic calculations were conducted based on the following equations and parameters collected from the literature (Tables 2 and 3): (1) mass balance of Fe and the quinone system: for Fe, the complexation with OH^- was considered with the stability constant collected from the literature[36] for the benzoquinone (Q) system, quinone, semiquinone (SQ, and SQ^-) (protonated and deprotonated), and hydroquinone (H_2Q, HQ^-, Q^{2-}) (protonated, partially deprotonated, and fully deprotonated); (2) electron balance: the electron levels of Fe(II) and Fe(III) were assigned as 1 and 0, while the electron levels of H_2Q, SQ^-, and Q were assigned as 2, 1, and 0, respectively; and (3) equilibrium: equilibrium of dissociation/association, complexation, and redox reactions was taken into account. For Fe(II) and Fe(III), the system was considered unsaturated and calculated, and then, the saturation index was calculated for the dissolution of $Fe(OH)_2$ and $Fe(OH)_3$; if the saturation index was above 1, the solubility product of $Fe(OH)_2$ and $Fe(OH)_3$ was included in the calculation.

Statistical Analysis. Statistical analysis was conducted with IBM SPSS Statistics (ver. 26, IBM Corp., Armonk, NY).

RESULTS AND DISCUSSION

Reductive Degradation of Triclosan by Semiquinone. When triclosan was mixed with H_2Q in a molar ratio of 1:1 (3 and 3 μM) at pH 3, 5, and 7, no triclosan degradation was observed under either oxic or anoxic conditions (Figure 1A).

Table 3. Major Equilibrium Constants Used in the Thermodynamic Calculations

reaction	equilibrium constant
dissociation	pK_a
$SQ = SQ^- + H^+$	4.1
$H_2Q = HQ^- + H^+$	10.16
$HQ^- = Q^{2-} + H^+$	12.02
complexation	stability constant ($\log K$)
$Fe^{3+} + OH^- = Fe(OH)^{2+}$	11.813
$Fe^{3+} + 2OH^- = Fe(OH)_2^+$	23.406
$Fe^{3+} + 3OH^- = Fe(OH)_3(aq)$	28.4
$Fe^{3+} + 4OH^- = Fe(OH)_4^-$	34.412
$Fe^{2+} + OH^- = Fe(OH)^+$	4.603
$Fe^{2+} + 2OH^- = Fe(OH)_2(aq)$	7.506
$Fe^{2+} + 3OH^- = Fe(OH)_3^-$	13.506
$Fe^{3+} + 4OH^- = Fe(OH)_4^{2-}$	10.012
dissolution	$\log K_{sp}$
$Fe(OH)_3 = Fe^{3+} + 3OH^-$	−15.9
$Fe(OH)_3 = Fe^{2+} + 2OH^-$	−37.11
redox reaction	E_H^0 (V)
$Q + e^- = SQ^-$	0.081
$Q + 2e^- = H_2Q$	0.045
$Fe^{3+} + e^- = Fe^{2+}$	0.776

Minor variations in the initial concentrations were likely due to experimental setup errors. This indicates that H_2Q cannot reduce triclosan within the experimental period (up to 288 h), likely because of the relatively high oxidation−reduction potentials of E_H^0 = 1091 and 1327 mV for SQ/H_2Q and SQ^- (dissociated ion of SQ)/H_2Q,[13,37] respectively, which will be discussed in more details below. In previous studies, HQs were assumed to degrade organohalogen,[2,38−40] and in this study, no reactions occurred between H_2Q and triclosan. Parallel measurement confirmed that H_2Q kept a constant concentration in the presence or absence of O_2 (Figure S4), as O_2 cannot oxidize H_2Q due to spin restriction.[41,42]

Remarkably, however, in the presence of $FeCl_3$, triclosan was degraded relatively quickly at pH 5 and 7 (Figure 1B). To get an overall assessment of the reaction rate, the triclosan degradation was fitted with pseudo-first-order kinetics with a rate constant of 0.0086 and 0.0097 h^{-1} and a half-life of 71.4−80.6 h ($p < 0.05$). The reaction rate constant is comparable to

https://doi.org/10.1021/acs.est.3c03981
Environ. Sci. Technol. XXXX, XXX, XXX−XXX

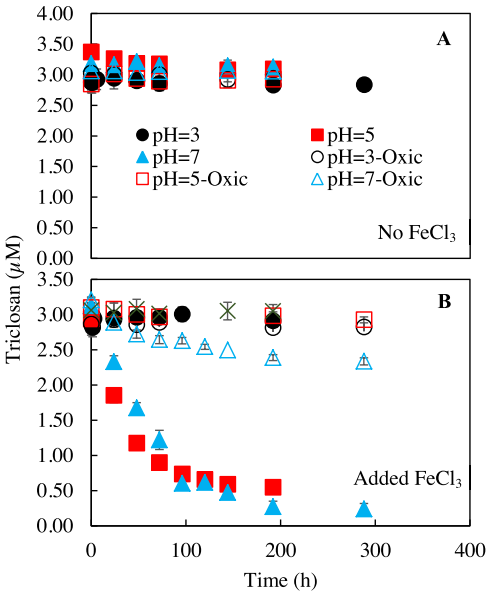

Figure 1. Kinetics for triclosan degradation in the reactions between hydrobenzoquinone (H_2Q) (3 μM) and triclosan (3 μM) in the absence (A) and presence (B) of $FeCl_3$ (3 μM). All reactions were conducted at pH 3, 5, and 7 and in anoxic (with dissolved O_2 < 10 μM) (filled symbols) and oxic conditions (dissolved O_2 = 200 μM) (open symbols). Error bars represent the standard deviation collected from triplicate measurements. Some error bars were too small to visualize.

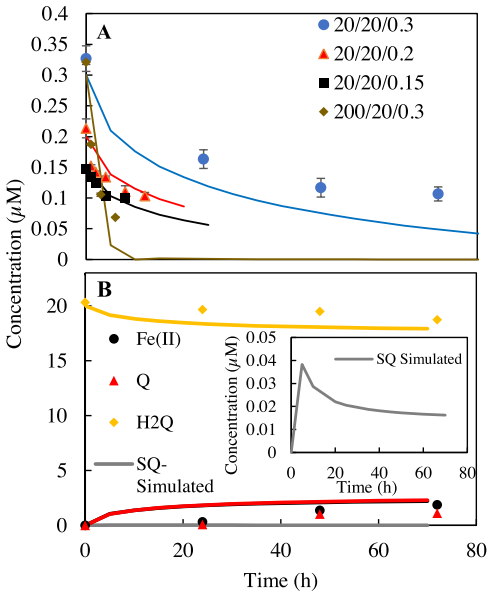

Figure 2. (A) Kinetics for the degradation of triclosan reacted with hydrobenzoquinone (H_2Q) and $FeCl_3$ in the absence of O_2 at pH 5 together with the simulation. Four different initial concentrations of $H_2Q/FeCl_3$/triclosan were used, including 20/20/0.3, 20/20/0.2, 20/20/0.15, and 200/20/0.15 μM, marked in the figure legends. Dots represent the measured results, while the lines represent the simulation. (B) Measured time-dependent concentrations of Fe(II), benzoquinone (Q), hydrobenzoquinone (H_2Q), and semibenzoquinone (SQ^-) in the system with the initial concentration of 20/20/0.3 μM $H_2Q/FeCl_3$/triclosan with the simulation. Error bars represent the standard deviation collected from triplicate measurements. Some error bars were too small to visualize.

the degradation of organohalogen by NOM or biochar, with the reported values of 0.00108−0.0105 h^{-1}.[3] Such degradation of triclosan was shut down at pH 3 or in the presence of saturated dissolved O_2. Additional control experiments eliminated the possibility of reactions between Fe(III) or Fe(II) and triclosan in the absence or presence of O_2 (Figure S4). Direct reactions confirmed that under anoxic conditions Q did not react with triclosan (Figure 1). Therefore, triclosan was predominantly degraded by products of a reaction between H_2Q and Fe(III), presumably SQ.[13,37] EPR signals corresponding to the C-centered radical (g = 2.0031) with adjacent oxygen were detected in a reaction system containing 300 μM H_2Q and 3 μM Fe(III) under anoxic conditions (Text S1 and Figure S5). No EPR signals (g = 2.0031) were detected in control experiments with only H_2Q or Fe(III). These results provide evidence for the formation of semiquinone radicals in the reaction system containing Fe(III) and H_2Q and its critical role in triclosan degradation.

The impact of the initial reactant concentration was examined with relatively low concentrations of triclosan (0.15, 0.2, 0.3 μM) reacted with H_2Q (20 μM) and Fe(III) (20 μM) (Figure 2). Under all of the different concentration sets, triclosan was degraded substantially. Triclosan degradation kinetics were fitted well by pseudo-first-order kinetics with a rate constant ranging 0.0475−0.0154 h^{-1} and half-life reduced from 45 to 14 h (p < 0.05) when the initial concentration of triclosan was reduced from 0.3 to 0.15 μM. For the system started with 20 μM $FeCl_3$ and 0.3 μM triclosan, when the initial H_2Q concentration was further increased to 200 μM, the reaction was further substantially expedited with the pseudo-first-order half-life of 2.8 h; within the reaction period (6 h), Fe(II) increased to 5.2 ± 0.04 μM and H_2Q reduced to 197.5 ± 1.56 μM (Q was increased to 3.15 ± 0.05 μM). The reduction of Fe(III) was consistent with previous data reported on a system consisting of only $FeCl_3$ and H_2Q.[13]

Furthermore, for the system containing 0.3 μM triclosan, 20 μM H_2Q, and 20 μM Fe(III), reaction byproducts of triclosan were analyzed by ESI-TOF-MS (Figure S6). Two major byproducts were detected: a dechlorinated phenoxyphenol (m/z = 252.982, $C_{12}H_8Cl_2O_2$) and a monochlorinated phenoxyphenol (m/z = 219.021, $C_{12}H_9ClO_2$). Monochlorinated phenoxyphenol was the major byproduct observed after 4 days of the reaction, based on the intensity of ESI-TOF-MS features. The analysis did not capture the fully dechlorinated phenoxyphenol (m/z = 182.0368, $C_{12}H_{10}O_2$), similar to our previous work on the degradation of triclosan by aqueous biochars.[3]

Kinetic Simulation and the Reaction Rate Constant. The dynamics of H_2Q, SQ, and Q were simulated for the system starting with 20 μM Fe(III) and 20 μM H_2Q (Figure 2). Due to the reversible oxidation of H_2Q by Fe(III), simulated SQ^- concentrations increased sharply in the first 10 h and approached the steady-state concentration of 34.1 nM. If saturated O_2 was present, SQ^- was further oxidized to Q and reduced significantly to less than 10^{-4} nM. In the presence of 1 μM O_2, SQ^- has fluctuations in the beginning stage of the reactions, and the steady-state concentration was ∼0.9 nM (Figure S7). These calculations supported the notion that SQ^-, much higher in concentration under anoxic conditions, is presumably responsible for the reductive dehalogenation of triclosan. The reaction between H_2Q/SQ^-, Fe(III), and triclosan was regulated by pH due to the speciation of SQ and H_2Q and their pH-dependent oxidation−reduction

https://doi.org/10.1021/acs.est.3c03981
Environ. Sci. Technol. XXXX, XXX, XXX−XXX

potential (Figure S8). Our results show that triclosan degradation was shut down when pH was reduced to 3 (Figure 1). The impaired degradation of triclosan at pH 3 can be attributed primarily to the elevated oxidation−reduction potentials (E_H) of Q/SQ^- (0.336 V at pH 3 compared to 0.218 V at pH 5), which potentially render the degradation of triclosan by SQ^- thermodynamically unfavorable. In the presence of oxygen, SQ^- undergoes rapid oxidation, resulting in the formation of Q.[13] Conversely, in the absence of oxygen, triclosan oxidizes SQ^- to Q. In the control reactions with triclosan and Fe(III)/Fe(II), no triclosan degradation was observed; reactions between triclosan degradation byproducts and Fe(III)/Fe(II) were not done due to lack of standards, and the reduction potentials for triclosan and triclosan degradation byproducts were not considered due to the lack of reliable reports or measurements.

Simulation for the kinetics of triclosan dehalogenation was conducted for systems with relatively lower triclosan concentration, where the consumption of SQ^- by triclosan degradation byproducts could be neglected. For the system with relatively low concentrations of triclosan (0.15, 0.2, 0.3 μM) reacted with H_2Q (20 μM) and Fe(III) (20 μM), the complete dehalogenation of 0.3 μM of triclosan required 1.8 μM electrons (2 mol e^-/1 mol Cl and 3 Cl in triclosan), equivalent to 1.8 μM H_2Q, below 10% of its initial concentration of 20 μM. As no standards were available for triclosan dehalogenation byproducts, H_2Q and Fe(III) were overdosed so that the consequent dehalogenation of byproducts could be ignored for the numerical fitting. From the kinetic perspective, based on the rate constant, the production and removal flux of SQ^- was around 400 μM/s, when triclosan would only consume at most 2.8×10^{-5} μM/s SQ^-, according to the 11 days's measured half-life of triclosan.

A least-squares fitting was conducted for the time-dependent concentrations of triclosan to determine the rate constant for the reaction between triclosan and SQ^-, considering all of the critical reactions occurring in the system (Table 1). The use of multiple sets of reactions with different initial concentrations ensured the rigorous fitting. Time-dependent concentrations of triclosan can be fitted well (Figure S9, normalized root-mean-square error (RMSE) = 0.14−0.46) with an overall third-order rate constant of 317 h^{-1} M^{-2} for the reactions between the SQ^- and triclosan at pH 5 (Figure 2A and Table 1). For the system with 200 μM H_2Q, 20 μM $FeCl_2$, and 0.3 μM triclosan, initially, the dynamics of Fe(III)/Fe(II) and H_2Q/Q were also fitted well (Figure 2B).

The rate constant for the reaction between SQ^- and triclosan was much higher than those obtained for the reactions between organohalogens and NOM/biochar.[31,40,43,44] For example, the reported pseudo-second-order reaction rate constant between NOM/biochar and organohalogen ranged 7.3×10^{-6}−1.48×10^{-6} M^{-1} h^{-1}.[31] As the semiquinone is usually a minor fraction of NOM/biochar thermodynamically, our results implied that the real reaction rate constant could also be higher than previously thought for the real reactive components in NOM/biochar if semiquinones rather than hydroquinones are real key components in NOM/biochar for dehalogenation, which requires further investigation to verify.

Thermodynamics vs Kinetics and Potential Importance of Other Semiquinones in Dehalogenation. Thermodynamically, the concentration of SQ^- is regulated by the redox conditions of the reaction system. Following the theme of calculation developed by Uchimiya et al.,[36] pH-dependent concentrations of SQ^- in the system with 20 μM H_2Q and 20 μM Q were calculated using a self-built Matlab code. SQ^- equilibrium concentration has a significant response to pH as a result of pH-dependent oxidation−reduction potentials (E_H) of reactions for Q and SQ^- (Figure S8). For the system with $FeCl_3$, the reactions are also constrained by the speciation of Fe and the solubility of produced minerals ($Fe(OH)_3$ and $Fe(OH)_2$). Considering the complexation of Fe(III)/Fe(II) with OH^- and the solubility product of $Fe(OH)_3$/$Fe(OH)_2$ complexes, the equilibrium concentrations of SQ^- were also calculated within the pH-dependent range 3.5×10^{-7}−3.5×10^{-3} μM, with the concentration of Fe(III) in solution being constrained by the precipitation of $Fe(OH)_3$ above a pH of 5.6 (Figure S10). The degradation of triclosan primarily resulted from the deprotonated semiquinone radical (pK_a of SQ = 4.1), prompting the selection of a pH range from 5 to 9 to simulate the semiquinone concentration, as triclosan did not undergo degradation at pH levels below 5. When the calculation was applied to the system containing 20 μM H_2Q and 20 μM $FeCl_3$, the equilibrium concentration of SQ^- was much lower than that calculated from the kinetic calculation (Figure 3). The reaction system, comprised of triclosan,

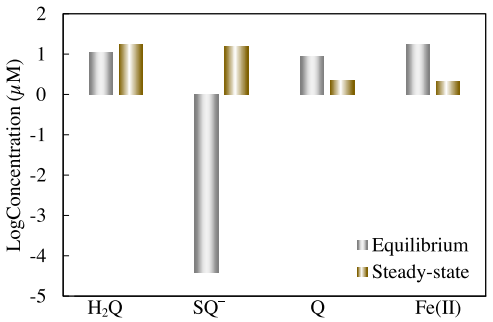

Figure 3. Comparison between the thermodynamic equilibrium and steady-state concentration (based on the kinetic simulation) of SQ^-, H_2Q, Q, and Fe(II) and thermodynamic equilibrium concentration for the system with 20 μM/20 μM H_2Q/$FeCl_3$ under the anoxic condition.

Fe(III), and H_2Q, with concentrations of 0.3, 20, and 20 μM, respectively, exhibited a notably elevated ΔG value of −306.8 kJ for the reaction between $FeCl_3$ and H_2Q. This calculation supported that the system had not achieved equilibrium at the conclusion of the specified reaction period. Based on oxidation−reduction potentials, the oxidation of SQ^- by Fe(III) is even more favored than the oxidation of H_2Q. However, the reactions of SQ^- with Fe(III) are relatively slower and kinetically limited,[13] with no reliable rate constant for the reactions between Q/SQ^- and Fe(III)/Fe(II) being available. Such a kinetic limit promotes the production of SQ^- due to the reaction between H_2Q and Fe(III) and subsequent reactions of SQ^- with organohalogen, with triclosan as a model compound in this study.

The critical role of SQ^- in the reductive degradation of triclosan could be partially driven by the relatively higher oxidation−reduction potential of SQ^-/H_2Q than Q/SQ^-. For most naturally occurring quinones, the oxidation−reduction potential of SQ^-/H_2Q was higher than Q/SQ^- at near-neutral pH. Song et al.[32] compiled data showing that the difference between the semiquinone/hydroquinone and quinone/semiquinone ranges between 300 and 500 mV for most of the

https://doi.org/10.1021/acs.est.3c03981
Environ. Sci. Technol. XXXX, XXX, XXX−XXX

quinone compounds at near-neutral pH. There are only a few exceptions, such as 2,6-methoxyl-3-methyl-1,4-benzoquinone, for which semiquinone/hydroquinone and quinone/semiquinone oxidation−reduction potentials are −290 and −110 mV, respectively.[41] Therefore, for most quinone systems, thermodynamically, semiquinone serves better as a reducing agent for reductive dehalogenation.[45,46] We verified that in the presence of only substituted hydrobenzoquinone or hydronaphthoquinone, triclosan was not degraded under anoxic conditions (20 μM hydroquinone and 0.3 μM triclosan at pH = 5) (Figure 4A). However, when 20 μM $FeCl_3$ was added to

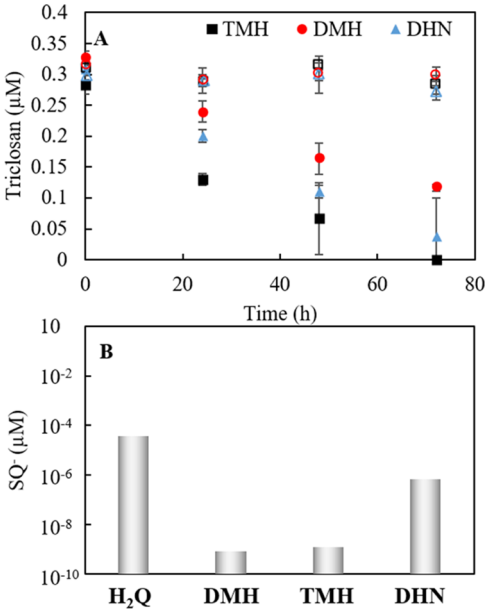

Figure 4. (A) Time-dependent triclosan concentration in anoxic reactions with substituted hydroquinones (HQs) (dimethyl hydroquinone (DMH), trimethyl hydroquinone (TMH), 1,2-dihydroxylnaphthlene (DHN)) with initial concentrations of 20/20/0.3 μM HQ/$FeCl_3$/triclosan, where open symbols represent the reaction system in the absence of Fe(III) and (B) calculated equilibrium semiquinone (SQ^-) concentrations in the system with different HQs in the system of 20/20/0.3 μM HQ/$FeCl_3$. The result for H_2Q is shown as a comparison. Error bars represent standard deviation collected from triplicate measurements. Some error bars were too small to visualize.

the system, triclosan was degraded with a pseudo-first-order half-life of 23.0−47.8 h (Figure 4A). Rate constants for dehalogenation reactions involving these hydroquinones in the presence of $FeCl_3$ were not available for kinetic simulation when thermodynamic equilibrium concentrations of semiquinones in these systems were determined to range 8.5×10^{-9}−6.7×10^{-7} μM (Figure 4B). The kinetic limit for the reaction between these semiquinones and Fe(III) also occurred similarly to SQ^- and enhanced the concentration of semiquinones. Furthermore, similar reactions involving other more widely used and naturally abundant hydroquinones (mitoxantrone and epigallocatechin) showed that triclosan could not be degraded in the absence of Fe(III), while the presence of Fe(III) enabled substantial degradation of triclosan within 12 days (Figure S11). While more detailed kinetic studies were not feasible due to the lack of data for the thermodynamics of multiple quinone groups present in these compounds, the above results confirm the critical role of semiquinones in the reductive dehalogenation of organohalogens for a broad group of quinones.

Environmental Implications. This study has demonstrated the critical role of SQs in reductive dehalogenation through experimental studies, kinetic fitting, and thermodynamics analysis. Although triclosan and H_2Q were used as model compounds, the observed importance can be applicable to an extensive range of quinone groups. As quinones have been assigned as the key groups in the NOM or biochar to promote the reductive degradation of organohalogen and other redox-sensitive organic compounds,[4−7] this finding has important implications for understanding the NOM/biochar-mediated reactions and optimization of their application in the water treatment and groundwater remediation. Semiquinone-type structures in biochar play a vital role in reducing contaminants like Cr(VI) to Cr(III) and act as redox sites to directly donate electrons.[47] Semiquinones in biochar also contribute to its electrical conductivity, facilitating electron transfer.[48] Additionally, they can act as electron mediators, accelerating electron transfer in various redox reactions.[2,3] Our results show that semiquinone is an effective electron donor in reductive dehalogenation in certain quinone systems. However, for a more extensive group of quinones, the addition of oxidants (such as Fe(III) or quinones themselves) together with hydroquinone will be crucial for triggering the reductive degradation of organohalogens and other toxic organic compounds.

■ ASSOCIATED CONTENT

Supporting Information

The Supporting Information is available free of charge at https://pubs.acs.org/doi/10.1021/acs.est.3c03981.

Additional experimental details; methods; and simulation and experimental results (PDF)

■ AUTHOR INFORMATION

Corresponding Author

Yu Yang − *Department of Civil and Environmental Engineering, University of Nevada, Reno, Reno, Nevada 89557, United States;* orcid.org/0000-0002-7568-0202; Email: yuy@unr.edu

Authors

Srinidhi Lokesh − *Department of Civil and Environmental Engineering, University of Nevada, Reno, Reno, Nevada 89557, United States*

Myron L. Lard − *Department of Chemistry, Louisiana State University, Baton Rouge, Louisiana 70803, United States*

Robert L. Cook − *Department of Chemistry, Louisiana State University, Baton Rouge, Louisiana 70803, United States;* orcid.org/0000-0003-4246-2951

Complete contact information is available at: https://pubs.acs.org/10.1021/acs.est.3c03981

Notes

The authors declare no competing financial interest.

■ ACKNOWLEDGMENTS

This study was supported by funding from the National Science Foundation Awards (Nos. NSF 1804209 and 2108270) and the National Institute of Environmental Health Sciences (NIEHS) Superfund Research Program (P42

ES013648). The authors acknowledge the shared instrument laboratory in the Department of Chemistry at UNR. They also acknowledge Dr. Stephen Spain and Dr. Janina Ruprecht from the Department of Chemistry for help with TOF-MS analysis. They are also grateful for the discussion with Dr. Pignatello at the Connecticut Agricultural Research Experimental Station and Dr. Prachi Joshi from the Department of Geosciences at the University of Tübingen.

REFERENCES

(1) Lefèvre, E.; Bossa, N.; Gardner, C. M.; Gehrke, G. E.; Cooper, E. M.; Stapleton, H. M.; Hsu-Kim, H.; Gunsch, C. K. Biochar and Activated Carbon Act as Promising Amendments for Promoting the Microbial Debromination of Tetrabromobisphenol A. *Water Res.* **2018**, *128*, 102−110.
(2) Yu, L.; Yuan, Y.; Tang, J.; Wang, Y.; Zhou, S. Biochar as an Electron Shuttle for Reductive Dechlorination of Pentachlorophenol by Geobacter Sulfurreducens. *Sci. Rep.* **2015**, *5*, No. 16221, DOI: 10.1038/srep16221.
(3) Lokesh, S.; Kim, J.; Zhou, Y.; Wu, D.; Pan, B.; Wang, X.; Behrens, S.; Huang, C.-H.; Yang, Y. Anaerobic Dehalogenation by Reduced Aqueous Biochars. *Environ. Sci. Technol.* **2020**, *54* (23), 15142−15150.
(4) Scott, D. T.; McKnight, D. M.; Blunt-Harris, E. L.; Kolesar, S. E.; Lovley, D. R. Quinone Moieties Act as Electron Acceptors in the Reduction of Humic Substances by Humics-Reducing Microorganisms. *Environ. Sci. Technol.* **1998**, *32* (19), 2984−2989.
(5) Aeschbacher, M.; Graf, C.; Schwarzenbach, R. P.; Sander, M. Antioxidant Properties of Humic Substances. *Environ. Sci. Technol.* **2012**, *46* (9), 4916−4925.
(6) Zhang, Y.; Xu, X.; Zhang, P.; Zhao, L.; Qiu, H.; Cao, X. Pyrolysis-Temperature Depended Quinone and Carbonyl Groups as the Electron Accepting Sites in Barley Grass Derived Biochar. *Chemosphere* **2019**, *232*, 273−280.
(7) Xu, Z.; Tsang, D. C. W. Redox-Induced Transformation of Potentially Toxic Elements with Organic Carbon in Soil. *Carbon Res.* **2022**, *1* (1), No. 9, DOI: 10.1007/s44246-022-00010-8.
(8) Perlinger, J. A.; Angst, W.; Schwarzenbach, R. P. Kinetics of the Reduction of Hexachloroethane by Juglone in Solutions Containing Hydrogen Sulfide. *Environ. Sci. Technol.* **1996**, *30* (12), 3408−3417.
(9) Xu, S.; Adhikari, D.; Huang, R.; Zhang, H.; Tang, Y.; Roden, E.; Yang, Y. Biochar-Facilitated Microbial Reduction of Hematite. *Environ. Sci. Technol.* **2016**, *50* (5), 2389−2395.
(10) Orsetti, S.; Laskov, C.; Haderlein, S. B. Electron Transfer between Iron Minerals and Quinones: Estimating the Reduction Potential of the Fe(II)-Goethite Surface from AQDS Speciation. *Environ. Sci. Technol.* **2013**, *47* (24), 14161−14168.
(11) Liu, C.; Zachara, J. M.; Foster, N. S.; Strickland, J. Kinetics of Reductive Dissolution of Hematite by Bioreduced Anthraquinone-2,6-disulfonate. *Environ. Sci. Technol.* **2007**, *41* (22), 7730−7735.
(12) Jiang, J.; Kappler, A. Kinetics of Microbial and Chemical Reduction of Humic Substances: Implications for Electron Shuttling. *Environ. Sci. Technol.* **2008**, *42* (10), 3563−3569.
(13) Jiang, C.; Garg, S.; Waite, T. D. Hydroquinone-Mediated Redox Cycling of Iron and Concomitant Oxidation of Hydroquinone in Oxic Waters under Acidic Conditions: Comparison with Iron−Natural Organic Matter Interactions. *Environ. Sci. Technol.* **2015**, *49* (24), 14076−14084.
(14) O'Loughlin, E. J. Effects of Electron Transfer Mediators on the Bioreduction of Lepidocrocite (γ-FeOOH) by Shewanella Putrefaciens CN32. *Environ. Sci. Technol.* **2008**, *42* (18), 6876−6882.
(15) Pracht, J.; Boenigk, J.; Isenbeck-Schröter, M.; Keppler, F.; Schöler, H. F. Abiotic Fe(III) Induced Mineralization of Phenolic Substances. *Chemosphere* **2001**, *44* (4), 613−619.
(16) Stack, A. G.; Eggleston, C. M.; Engelhard, M. H. Reaction of Hydroquinone with Hematite. *J. Colloid Interface Sci.* **2004**, *274* (2), 433−441.
(17) Wiseman, L. R.; Spencer, C. M. Mitoxantrone. *Drugs Aging* **1997**, *10* (6), 473−485.
(18) Lin, R. D.; Steinmetz, N. F. Tobacco Mosaic Virus Delivery of Mitoxantrone for Cancer Therapy. *Nanoscale* **2018**, *10* (34), 16307−16313, DOI: 10.1039/C8NR04142C.
(19) Mei, K.-C.; Liao, Y.-P.; Jiang, J.; Chiang, M.; Khazaieli, M.; Liu, X.; Wang, X.; Liu, Q.; Chang, C. H.; Zhang, X.; Li, J.; Ji, Y.; Melano, B.; Telesca, D.; Xia, T.; Meng, H.; Nel, A. E. Liposomal Delivery of Mitoxantrone and a Cholesteryl Indoximod Prodrug Provides Effective Chemo-Immunotherapy in Multiple Solid Tumors. *ACS Nano* **2020**, *14* (10), 13343−13366.
(20) Du, G. J.; Zhang, Z.; Wen, X. D.; Yu, C.; Calway, T.; Yuan, C. S.; Wang, C. Z. Epigallocatechin Gallate (EGCG) Is the Most Effective Cancer Chemopreventive Polyphenol in Green Tea. *Nutrients* **2012**, *4* (11), 1679−1691.
(21) Nagle, D. G.; Ferreira, D.; Zhou, Y.-D. Epigallocatechin-3-Gallate (EGCG): Chemical and Biomedical Perspectives. *Phytochemistry* **2006**, *67* (17), 1849−1855.
(22) Khan, N.; Afaq, F.; Saleem, M.; Ahmad, N.; Mukhtar, H. Targeting Multiple Signaling Pathways by Green Tea Polyphenol (−)-Epigallocatechin-3-Gallate. *Cancer Res.* **2006**, *66* (5), 2500−2505.
(23) Almatroodi, S. A.; Almatroudi, A.; Khan, A. A.; Alhumaydhi, F. A.; Alsahli, M. A.; Rahmani, A. H. Potential Therapeutic Targets of Epigallocatechin Gallate (EGCG), the Most Abundant Catechin in Green Tea, and Its Role in the Therapy of Various Types of Cancer. *Molecules* **2020**, *25* (14), No. 3146.
(24) Gledhill, M.; Buck, K. The Organic Complexation of Iron in the Marine Environment: A Review. *Front. Microbiol.* **2012**, *3*, No. 69, DOI: 10.3389/fmicb.2012.00069.
(25) Johnson, K. S.; Gordon, R. M.; Coale, K. H. What Controls Dissolved Iron Concentrations in the World Ocean? *Mar. Chem.* **1997**, *57* (3), 137−161.
(26) https://www.lenntech.com/periodic/water/iron/iron-and-water.htm#ixzz88bt0GDWh (accessed July 26, 2023).
(27) Patzner, M. S.; Mueller, C. W.; Malusova, M.; Baur, M.; Nikeleit, V.; Scholten, T.; Hoeschen, C.; Byrne, J. M.; Borch, T.; Kappler, A.; Bryce, C. Iron Mineral Dissolution Releases Iron and Associated Organic Carbon during Permafrost Thaw. *Nat. Commun.* **2020**, *11* (1), No. 6329.
(28) Garg, S.; Jiang, C.; Waite, T. D. Mechanistic Insights into Iron Redox Transformations in the Presence of Natural Organic Matter: Impact of PH and Light. *Geochim. Cosmochim. Acta* **2015**, *165*, 14−34, DOI: 10.1016/j.gca.2015.05.010.
(29) Yamazaki, I.; Ohnishi, T. One-Electron-Transfer Reactions in Biochemical Systems I. Kinetic Analysis of the Oxidation-Reduction Equilibrium between Quinol-Quinone and Ferro-Ferricytochrome c. *Biochim. Biophys. Acta, Biophys. Incl. Photosynth.* **1966**, *112* (3), 469−481.
(30) Yuan, X.; Pham, A. N.; Miller, C. J.; Waite, T. D. Copper-Catalyzed Hydroquinone Oxidation and Associated Redox Cycling of Copper under Conditions Typical of Natural Saline Waters. *Environ. Sci. Technol.* **2013**, *47* (15), 8355−8364.
(31) Kappler, A.; Haderlein, S. B. Natural Organic Matter as Reductant for Chlorinated Aliphatic Pollutants. *Environ. Sci. Technol.* **2003**, *37* (12), 2714−2719.
(32) Song, Y.; Buettner, G. R. Thermodynamic and Kinetic Considerations for the Reaction of Semiquinone Radicals to Form Superoxide and Hydrogen Peroxide. *Free Radiccal Biol. Med.* **2010**, *49* (6), 919−962.
(33) Meisel, D. Free Energy Correlation of Rate Constants for Electron Transfer between Organic Systems in Aqueous Solutions. *Chem. Phys. Lett.* **1975**, *34* (2), 263−266.
(34) Bielski, B.; Cabelli, D.; Arudi, R. L.; Ross, A. Reactivity of HO2/O−2 Radicals in Aqueous Solution. *J. Phys. Chem. Ref. Data* **1985**, *14* (4), 1041−1051.
(35) Rush, J. D.; Bielski, B. H. Pulse Radiolytic Studies of the Reaction of Perhydroxyl/Superoxide O2-with Iron (II)/Iron (III) Ions. The Reactivity of HO2/O2-with Ferric Ions and Its Implication

https://doi.org/10.1021/acs.est.3c03981
Environ. Sci. Technol. XXXX, XXX, XXX−XXX

on the Occurrence of the Haber-Weiss Reaction. *J. Phys. Chem. A* **1985**, *89* (23), 5062−5066.
(36) Uchimiya, M.; Stone, A. T. Reversible Redox Chemistry of Quinones: Impact on Biogeochemical Cycles. *Chemosphere* **2009**, *77* (4), 451−458.
(37) Garg, S.; Ito, H.; Rose, A. L.; Waite, T. D. Mechanism and Kinetics of Dark Iron Redox Transformations in Previously Photolyzed Acidic Natural Organic Matter Solutions. *Environ. Sci. Technol.* **2013**, *47* (4), 1861−1869.
(38) Curtis, G.; Reinhard, M. Reductive dehalogenation of hexachlorethane, carbon-tetrachloride, and bromoform by anthrahydroquinone disulfonate and humic-acid. *Environ. Sci. Technol.* **1994**, *28*, 2393−2401.
(39) Warner, J. R.; Copley, S. D. Pre-Steady-State Kinetic Studies of the Reductive Dehalogenation Catalyzed by Tetrachlorohydroquinone Dehalogenase. *Biochemistry* **2007**, *46* (45), 13211−13222.
(40) Collins, R.; Picardal, F. Enhanced Anaerobic Transformations of Carbon Tetrachloride by Soil Organic Matter. *Environ. Toxicol. Chem.* **1999**, *18* (12), 2703−2710.
(41) Roginsky, V.; Barsukova, T. Kinetics of Oxidation of Hydroquinones by Molecular Oxygen. Effect of Superoxide Dismutase. *J. Chem. Soc., Perkin Trans. 2* **2000**, No. 7, 1575−1582.
(42) Miller, D. M.; Buettner, G. R.; Aust, S. D. Transition metals as catalysts of "autoxidation" reactions. *Free Radical Biol. Med.* **1990**, *8* (1), 95−108.
(43) Barkovskii, A. L.; Adriaens, P. Impact of humic constituents on microbial dechlorination of polychlorinated dioxins. *Environ. Toxicol. Chem.* **1998**, *17* (6), 1013−1020.
(44) Aulenta, F.; Maio, V. D.; Ferri, T.; Majone, M. The Humic Acid Analogue Antraquinone-2,6-Disulfonate (AQDS) Serves as an Electron Shuttle in the Electricity-Driven Microbial Dechlorination of Trichloroethene to Cis-Dichloroethene. *Bioresour. Technol.* **2010**, *101* (24), 9728−9733.
(45) Kristensen, S. B.; van Mourik, T.; Pedersen, T. B.; Sørensen, J. L.; Muff, J. Simulation of Electrochemical Properties of Naturally Occurring Quinones. *Sci. Rep.* **2020**, *10* (1), No. 13571.
(46) Huynh, M. T.; Anson, C. W.; Cavell, A. C.; Stahl, S. S.; Hammes-Schiffer, S. Quinone 1 e− and 2 e−/2 H+ Reduction Potentials: Identification and Analysis of Deviations from Systematic Scaling Relationships. *J. Am. Chem. Soc.* **2016**, *138* (49), 15903−15910.
(47) Zhao, N.; Yin, Z.; Liu, F.; Zhang, M.; Lv, Y.; Hao, Z.; Pan, G.; Zhang, J. Environmentally Persistent Free Radicals Mediated Removal of Cr(VI) from Highly Saline Water by Corn Straw Biochars. *Bioresour. Technol.* **2018**, *260*, 294−301.
(48) Sun, T.; Levin, B. D. A.; Guzman, J. J. L.; Enders, A.; Muller, D. A.; Angenent, L. T.; Lehmann, J. Rapid Electron Transfer by the Carbon Matrix in Natural Pyrogenic Carbon. *Nat. Commun.* **2017**, *8* (1), No. 14873.

https://doi.org/10.1021/acs.est.3c03981
Environ. Sci. Technol. XXXX, XXX, XXX−XXX